

Realtime Few-shot Portrait Stylization Based On Geometric Alignment

Xinrui Wang^{1,3} Zhuoru Li² Xiao Zhou⁴ Yusuke Iwasawa¹ Yutaka Matsuo¹
¹The University of Tokyo, ²Project HAT, ³Japan Computer Vision, ⁴Hefei Normal University

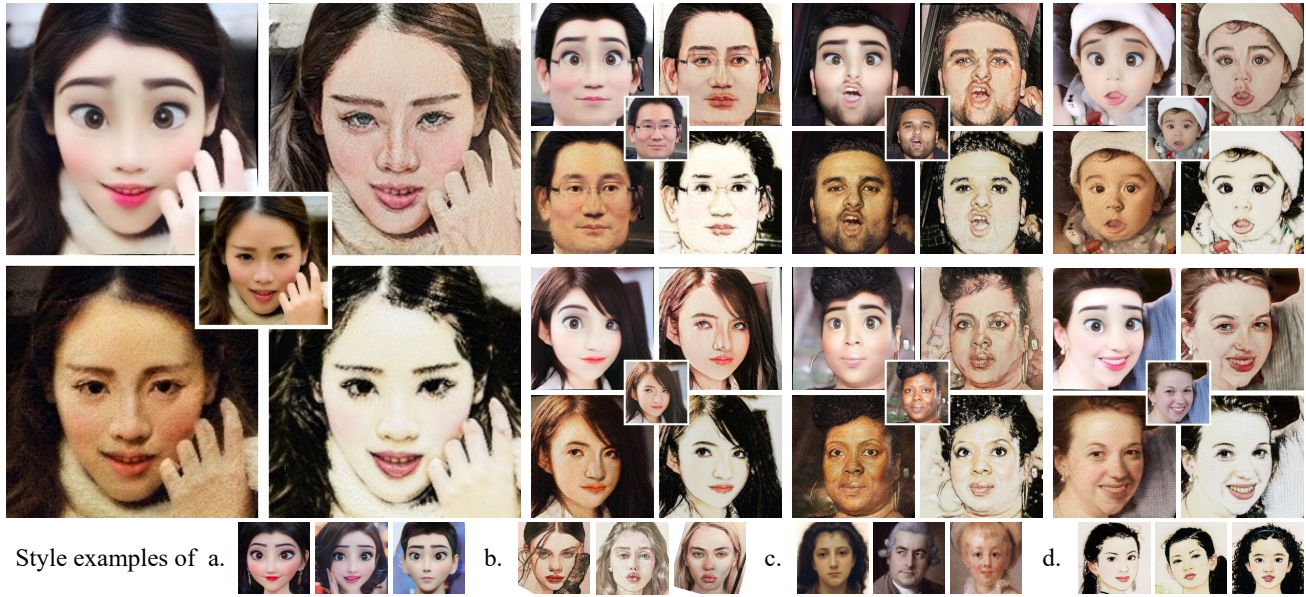


Figure 1. Our proposed method synthesizes vivid high-quality stylized portraits with limited style examples. The four styles are a:animation style in the left top, b: watercolor style in the right top, c:oil paint style in the left bottom and d:ink paint style in the right bottom.

Abstract

This paper presents a portrait stylization method designed for real-time mobile applications with limited style examples available. Previous learning based stylization methods suffer from the geometric and semantic gaps between portrait domain and style domain, which obstacles the style information to be correctly transferred to the portrait images, leading to poor stylization quality. Based on the geometric prior of human facial attributions, we propose to utilize geometric alignment to tackle this issue.

Firstly, we apply Thin-Plate-Spline (TPS) on feature maps in the generator network and also directly to style images in pixel space, generating aligned portrait-style image pairs with identical landmarks, which closes the geometric gaps between two domains. Secondly, adversarial learning maps the textures and colors of portrait images to the style domain. Finally, geometric aware cycle consistency preserves the content and identity information unchanged, and deformation invariant constraint suppresses artifacts and distortions. Qualitative and quantitative comparison validate our method outperforms existing methods, and experiments proof our method could be trained with limited

style examples (~ 100 or less) in real-time (more than 40 FPS) on mobile devices. Ablation study demonstrates the effectiveness of each component in the framework.

1. Introduction

Portrait stylization brings vivid artistic visual effects to human face photos from the style examples. The recent emerging of social networks and short video applications such as TikTok and Snapchat, and the convenience to novice users brought by mobile devices popularize portrait stylization, making it a high-demanding topic in both academia and industry. However, current methods in the industry are mainly trained on large scale manual created paired dataset, which is labor-intensive and financially expensive to prepare, costing enormous time and efforts of trained artists.

To automate the stylization process and reduce the number of style examples needed, Convolution Neural Networks (CNN) are adopted on neural style transfer [4, 12] and portraits stylization tasks [33] by transferring textures and colors, but they are less suitable for maintaining semantic consistency, resulting in drastic appearance changes. Generative Adversarial Network (GAN) [5] introduces new

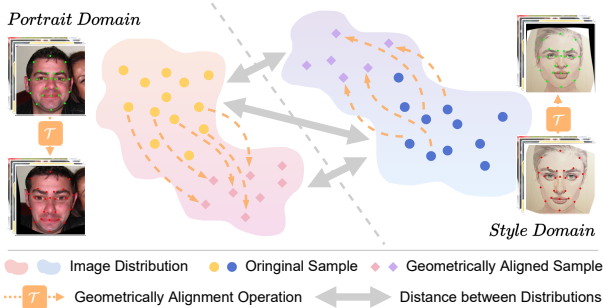


Figure 2. The proposed geometric alignment effectively closes the gap between portrait domain and the style domain.

mechanisms for image synthesis. [11, 41] learn to map paired-images from one domain to another, but the accessibility of paired data makes them less practical. [55] proposes cycle-consistency for unpaired image-to-image (I2I) translation, yet it is based on a strong assumption that the source domain and the target domain are semantically similar, making it unsuitable for situations where geometric gaps exist between two domains. [14, 15] are designed to synthesize high-quality and high-resolution images and also tailored for I2I translation and stylization [31, 47]. Nonetheless, the demand of large scale training data and the precision of StyleGAN inversion limit the application scenarios. Diffusion models [8, 36] recently achieved impressive results in generating high-quality samples with various styles. However, the high synthesis quality is at the cost of high computational complexity in both training and inference, making them unaffordable in real-time application.

While geometric and semantic misalignment of portraits and style images pose non-trivial challenges to previous methods, we notice that portrait images are highly structured in that everyone has the same facial features: the eyebrows, eyes, nose and mouth. This geometric prior is utilized to align style-portrait image pairs so as to close the geometric gap between two domains for stylization. [34, 38] perform exemplar based stylization, making them less general to diverse use cases and unsuitable for end-to-end inference. [54] learns dense correspondence for I2I translation, yet the large training dataset and high computational complexity make it unaffordable for real-time tasks.

To tackle the above mentioned issues, we propose to explicitly integrate geometric alignment into a learning framework with differentiable TPS modules. As shown in figure 2, face landmarks of portraits [44] and style faces [48] are detected to guide TPS [1] for geometric alignment. In the generation stage, TPS modules are integrated in the generator for feature space warping, allowing for the synthesis of both geometrically deformed and geometrically invariant samples. In the discrimination stage, TPS is directly applied to the style images to get geometric aligned portrait-style image pairs, helping discriminator focus on

corresponding facial features. Cycle-consistency is applied on aligned image pairs as content constraint, and spatial correlative loss [53] imposed on the generator suppresses artifacts and keeps synthesis results deformation invariant.

The geometric alignment enables our framework to be optimized in a semantic corresponded manner, effectively improved the synthesis quality and reduced artifacts caused by domain-wise geometric gap. It also allows for feature-space editing and facilitates few-shot stylization with limited style samples (~ 100 or less). The method is trained on variety of artistic styles and tested on human faces in diverse scenarios. Experiments show our method synthesizes high-quality stylized results in realtime, enabling it to be applied in mobile applications. We also compare our method with existing methods to illustrate our superiority. Finally, ablation studies are conducted to reveal the effect of each component. To conclude, our contributions are as follows:

- We propose to utilize the structure of portrait images to geometrically align the portrait-style image pairs and close the gap between two domains, enabling the stylization to be learned with an I2I translation framework in a semantic corresponding manner.
- We design a cycle-consistency framework with TPS integrated to train light-weighted stylization network and facilitate spatial editing. To the best of our knowledge, it's the first learning-based method that can be trained with less than 100 style samples and inference at realtime on mobile devices.
- Qualitative comparison, quantitative evaluation and user study are conducted to show that our method outperforms previous methods. Ablation study demonstrates the effectiveness of each component.

2. Related Work

2.1. Non-photorealistic Rendering

Non-photorealistic Rendering (NPR) bring artistic styles to photos. [26, 45] realize pencil sketching effects by iteratively optimizing the local statistic pattern of pencil sketch. oil paint style has been studied with texture synthesis methods [6, 39] and then CNN based methods [4, 12]. Animation style is also extensively explored with filtering based method [20, 40] and end-to-end neural network [2, 42], covering the use cases of portraits [42, 46], sceneries [2, 42], and even videos [40]. I2I translation based NPR have also been widely studied. [4, 24] adopt iterative optimization for neural style transfer (NST). [25, 56] use differentiable renders imitating the brush strokes of human artist for neural painting. [32] utilizes adversarial learning to learn to stylize images from a dataset instead of a single example. [11, 55] introduced I2I translation to NPR tasks, enabled inter-domain any to any transformation.

While a two-step align-stylize process is also adopted by [34], it stylizes portrait images by matching the multi-

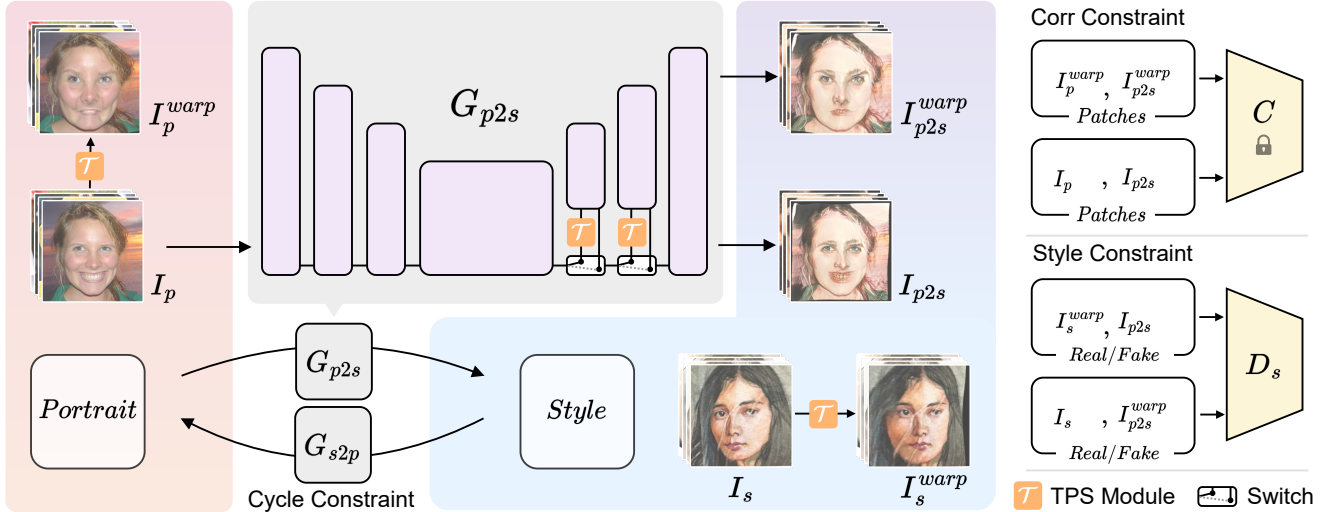


Figure 3. A single direction transformation of the framework. I_p and I_s represent portrait and style images, I_{p2s} and I_{p2s}^{warp} represent stylization results, I_s^{warp} and I_p^{warp} represent TPS warped results, C represents pretrained network to calculate spatial correlative loss.

scale local statistic of the style image. In this work, we take advantage of the flexible I2I translation framework for portrait stylization. By combining a cycle-consistency framework with geometric alignment strategy, our method could be trained with limited style samples, which largely improves the applicability to real-world applications where training data are hard to access.

2.2. Vision Generative Models

Generative Adversarial Network (GAN) [5] synthesizes samples with the same distribution as the training dataset by solving a min-max problem between a generator network and a discriminator network, forcing the generated samples to be indistinguishable from real data. It is capable of generating high quality samples [14, 15] and being adopted to downstream tasks [30, 32, 49, 50]. Variational autoencoders (VAE) [19] enable efficient density estimation, but sample quality is not on par with GANs. Diffusion models [8, 36] recently achieved state-of-the-art performance on both sample quality [3] and density estimation [17] by modeling the diffusion process into a Markov chain. However, its demand for training data and computation complexity are high. To enable real-time inference on mobile devices, we adopt an adversarial learning paradigm in the I2I framework to train a light-weighted generator network for portrait stylization.

2.3. Image-to-Image Translation

Image-to-Image Translation [9, 11, 21, 55] aims at translating images from a source domain to another target domain. It is widely adopted in image quality enhancement [10], stylizing photos into paintings [12, 32], cartoon images [2, 42] and sketches [23], as well as grayscale photo colorization [51] and sketch colorization [49, 50]. Early I2I translation methods perform single directional translation [11, 12]. Bi-directional models [55] are then introduced

for translation between unpaired images. Disentangle models [9, 21] are designed to separate content information and style information from images, realizing style translation with content information unchanged. Different from previous bi-directional methods, we utilize the cycle-consistency to constraint the semantic content, and only focus on the single-directional portrait to style transformation.

3. Method

We illustrate the overview of proposed framework in figure 3. It takes images and corresponding landmarks of both portrait and style domains as input. We denote the portrait image, the style image, the portrait landmarks, and the style landmarks as I_p , I_s , L_p , L_s respectively. A single direction portrait-to-style transformation is as follows:

In the geometric warping branch, the generator G_{p2s} warps the feature maps from L_p to L_s using integrated multi-scale TPS and synthesizes the deformed result I_{p2s}^{warp} , which has the identical landmark as I_s . In the geometric invariant branch, G_{p2s} directly synthesizes geometrically unchanged I_{p2s} . TPS is applied to I_s to warp it from L_s to L_p and get I_s^{warp} , which has identical landmark as I_{p2s} .

The two aligned image pairs are fed into the discriminator D_s to adversarially learn the mapping from the portrait domain to the style domain. A region-aware feature matching loss is adopted to force the synthesized samples to match the statistics of style samples in aligned regions. We also apply spatial correlative loss between the two image pairs with identical landmarks, I_{p2s} and I_p , I_{p2s}^{warp} and I_p^{warp} , to keep the generator deformation invariant.

The style-to-portrait transformation is strictly symmetric, and geometric aligned cycle-consistency loss guarantees the translation cycle brings image back to the original ones. In the following sections, we introduce each compo-

ment of the proposed framework in detail.

3.1. Multi-scale TPS assisted generation

To fulfill geometric deformation and edition, we integrate the TPS transformation [1] in the generator. TPS transformation is a nonlinear transformation that allows representing complex geometric deformation. Given corresponding landmarks of two images, we can warp one to the other with minimum distortion by applying TPS transformation \mathcal{F} :

$$\min \iint_{R^2} \left(\left(\frac{\partial^2 \mathcal{F}}{\partial x^2} \right)^2 + 2 \left(\frac{\partial^2 \mathcal{F}}{\partial x \partial y} \right)^2 + \left(\frac{\partial^2 \mathcal{F}}{\partial y^2} \right)^2 \right) dx dy, \quad (1)$$

s.t. $\mathcal{F}(P_i^S) = P_i^D, \quad i = 1, 2, \dots, N,$

where P_i^S and P_i^D represent the landmarks of the source image and the target image respectively. For each source-target image pair, there are $K \times N$ landmarks detected by predefined facial landmark detector. Every N pairs (we set $N = 10$ for our method) of landmarks generate one TPS transformation from \mathbf{S} to \mathbf{D} . According to the derivation of equation 1, the k^{th} TPS transformation is obtained as below:

$$\mathcal{F}_k(p) = A_k \begin{bmatrix} p \\ \mathbf{1} \end{bmatrix} + \sum_{i=1}^N w_{ki} U(\|P_{ki}^D - p\|_2), \quad (2)$$

where $p = (x, y)^T$ represents pixel coordinates, $A_k \in \mathcal{R}^{2 \times 3}$ and $w_{ki} \in \mathcal{R}^{2 \times 1}$ are the TPS coefficients obtained by solving Eq. (1), $U(r)$ is the radial basis function representing the influence of each landmark on the pixel at p :

$$U(r) = r^2 \log r^2. \quad (3)$$

We adopt an U-Net like generator. In the geometric warping branch, we integrate TPS modules in every down-sampled scales to warp the feature maps. Each warped feature map are upsampled and concatenated to the next scale, until the 3 channels RGB images are synthesized. In the geometric invariant branch, the TPS modules are skipped and the stylization results are directly synthesized by the generator. When doing inference, the stylization results are synthesized directly by the generator without TPS, and TPS is used only when geometric editing is desired.

3.2. Geometric aware discrimination

The Adversarial loss of vanilla CycleGAN imposes constraint on the high-level semantic space, making it less controllable and easily affected by geometric distortion. In order to realize stylization and meanwhile preserve the identity and geometric appearance, we align I_{p2s} and I_s^{warp} , I_{p2s}^{warp} and I_s as geometric identical portrait-style image pairs, and feed them to the discriminator for geometric aware discrimination. The adversarial loss for the portrait

to style transformation $\min_{G_{p2s}} \max_{D_s} \mathcal{L}_{GAN}(G_{p2s}, D_s)$ is expressed as below:

$$\mathcal{L}_{GAN}(G_{p2s}, D_s) = \mathbb{E}_{I_s \sim p_{data}(I_s)} [\log D_s(I_s)] + \mathbb{E}_{I_p \sim p_{data}(I_p)} [\log(1 - D_s(G_{p2s}(I_p)))] \quad (4)$$

We also adopt an adversarial loss for the symmetrical transformation: $\min_{G_{s2p}} \max_{D_p} \mathcal{L}_{GAN}(G_{s2p}, D_p)$.

Feature matching loss is adopted to stabilize training and improve synthesis quality. While previous methods match the statistics on the channel dimensions and neglect spatial information, we propose to reduce the channel dimension and matches the statistics of the spatial dimension on the intermediate layer of the discriminator. The proposed geometric aware feature matching loss is presented as below:

$$\mathcal{L}_{FM}(G_{p2s}, D_s) = [\|D_s^i(I_s) - D_s^i(G_{p2s}(I_p))\|_1] \quad (5)$$

where i represent the i_{th} feature map of the discriminator. As the eyes, nose and mouth regions represent most of the information in the human face, it can fully exploit the aligned spatial information to improve the synthesis quality. We also adopt symmetric loss on the style to portrait transformation. In the experiments, we illustrate the geometric-aware feature-matching loss outperforms the vanilla feature-matching loss.

3.3. Deformation invariant constraint

Directly applying TPS on images results in aliasing artifacts and distortions, while our proposed multi-scale TPS generator eases this problem, as the pixel errors caused by warping low resolutions feature maps is much lower than warping high resolution images. To further improve synthesis quality, we impose learning objectives on the generator so as to learn to smooth the synthesized samples.

We adopt spatial correlative loss as the deformation invariant constraint between I_p and I_{p2s} , I_p^{warp} and I_{p2s}^{warp} . By exploiting the spatial patterns of self-similarity and adopting contrastive learning criteria, it is able to preserving scene structure consistency while allowing appearance changes, and effectively guides the generator to synthesize distortion and artifacts free results. We express the spatial correlative loss as below, which is calculated based on features extracted from image patches by the trained network:

$$\mathcal{L}_C = -\log \frac{e^{sim(p, p^+)/\tau}}{e^{sim(p, p^+)/\tau} + \sum_{k=1}^K e^{sim(p, p_k^-)/\tau}} \quad (6)$$

where p denotes the spatially correlative map of queried patch, and p^+ and p^- are positive and negative patches respectively. $sim(p, p^+) = p^T p^+ / \|p\| \|p^+\|$ is the cosine similarity between two spatially-correlative maps, and τ is a temperature parameter, which is set to 0.07 in this paper. We show the comparisons between different losses as deformation invariant constraint in the experiments.



Figure 4. Illustration of stylization results. From top to bottom: portrait images, animation style results, watercolor style results, oil paint style results and ink paint style results. Zoom in for details.

3.4. Full model

We adopt a cycle-consistency framework for the portrait stylization method. To avoid the sub-optimal results caused by large geometric gaps between two domains, we only apply cycle-consistency loss on the geometric invariant branch, where the image triplets involved in calculating cycle-consistency loss have identical landmarks. Different from previous methods that directly minimize the L1 loss on images, we adopt LPIPS loss [52] which accelerates the convergence and improves synthesis quality. We show the cycle-consistency as below:

$$\begin{aligned} \mathcal{L}_{\text{Cyc}} = & \mathbb{E}_{I_s \sim p_{\text{data}}(I_s)} \|F_{\text{LPIPS}}(G_{p2s}(G_{s2p}(I_s))) - F_{\text{LPIPS}}(I_s)\|_1 \\ & + \mathbb{E}_{I_p \sim p_{\text{data}}(I_p)} \|F_{\text{LPIPS}}(G_{s2p}(G_{p2s}(I_p))) - F_{\text{LPIPS}}(I_p)\|_1 \end{aligned} \quad (7)$$

The full model is trained by jointly minimizing the following losses:

$$\begin{aligned} \mathcal{L}(G_{p2s}, G_{s2p}, D_s, D_p) = & \mathcal{L}_{\text{GAN}}(G_{p2s}, G_{s2p}, D_s, D_p) \\ & + \lambda_1 * \mathcal{L}_{\text{FM}}(G_{p2s}, G_{s2p}, D_s, D_p) \\ & + \lambda_2 * \mathcal{L}_C + \lambda_3 * \mathcal{L}_{\text{Cyc}} \end{aligned} \quad (8)$$

Where λ_1 , λ_2 and λ_3 represent the weight of each term. (8)

4. Experiment

4.1. Experiment Setup

Implementation. The proposed method is implemented by Pytorch [29]. We describe the generator and discriminator architectures in the supplementary material. Adaptive discriminator augmentation [13] is adopted to prevent overfitting. The learning rate and batch size are set to be $1 * 10^{-4}$ and 1. Adam optimizer [18] is adopted to optimize both networks, Training stops at 500000 step or on convergence.

Hyper-Parameters. λ_1 , λ_2 and λ_3 are set to be 1, 1, and 10 respectively. Further discussion of hyper-parameters is included in the supplementary material.



Figure 5. Examples of different styles in the dataset. From left to right: animation, water color, oil paint and ink paint.

Table 1. Inference time on different devices

Device	GPU	CPU	Mobilephone
Large Model	13.6ms	197.5ms	152.85ms
Small Model	3.6ms	26.8ms	23.5ms

Dataset. We train the stylization network on 4 different styles. The face area of images are cropped out and resized to 256*256 resolution for all datasets. For the portrait data, we collect 10000 images from the FFHQ dataset [14]. For the oil paint style, we collect 300 facial images from the Wikiart dataset [27]. For the animation style, the water color style and the ink paint style, we collect 820 images, 64 images and 34 images respectively. All datasets will be made publicly available to facilitate further studies.

Evaluation Metrics. In the qualitative comparison, we show the results of our proposed method and four previous methods with qualitative analysis. In quantitative evaluation, we adopt Art-FID [43] as the criterion, which represents the distance between the portrait distribution and the style distribution. In the user study, we invite 30 participants to select the best stylization results from 64 sets of images, among the results of our method and previous methods.

Baselines. We compare our framework with CycleGAN [55] that represents unpaired I2I translation, DRIT++ [22] that represents example based generation, U-GAT-IT [16] that represents portrait stylization and AgileGAN [35] that

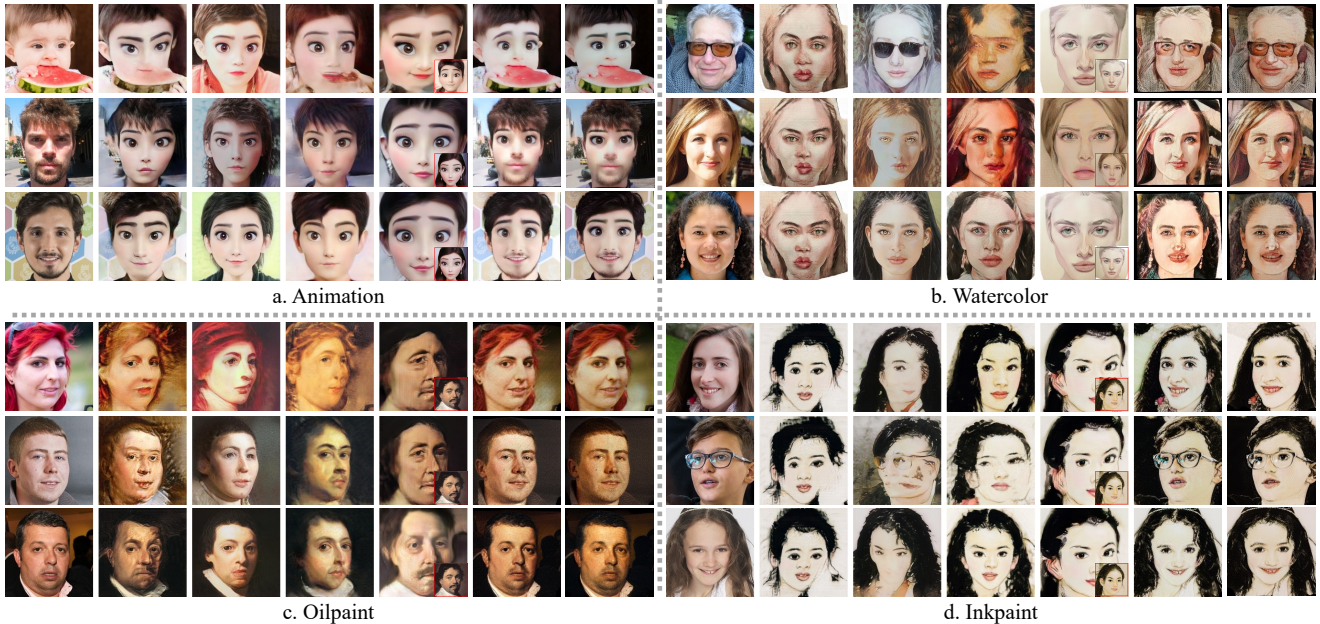


Figure 6. Qualitative comparison. For each style, we represent the portrait images and the results of CycleGAN, AgileGAN, UGATIT, DRIT++, our large model and our small model from left to right. Zoom in for details.

Table 2. Quantitative performance evaluated by Art-FID. Red and Blue represents the performance in the 1st and 2nd place respectively.

Methods	CycleGAN	DRIT++	U-GAT-IT	AgileGAN	Ours(large)	Ours(small)
Animation	81.74	122.28	93.97	85.96	85.80	80.23
Watercolor	355.34	426.56	257.78	312.12	246.97	251.54
Oilpaint	152.86	355.65	195.58	204.65	137.71	160.84
Inkpaint	304.89	306.74	271.70	306.15	269.06	274.25

Table 3. Cosine distance between different image distributions.

Domains	I_p and I_s	I_p and I_{s2p}	I_s and I_{p2s}
Distance	0.243	0.211	0.214

represents StyleGAN inversion. All compared methods are trained with the official implementations, default settings, and the same dataset used to train our proposed method.

Illustration of Different Styles. In figure 5, we show the examples of four different style in our dataset. Four models are trained on each dataset respectively. The stylization results of different models are shown in figure 4

Time Performance. We train both large and small models with proposed framework respectively, and evaluate the inference speed on three devices: AMD Ryzen 5800h laptop cpu, Nvidia RTX3060 laptop gpu and Qualcomm Snapdragon 855 mobile SOC. As is shown in table 1, the large model inferences at real-time on GPU, while the small model inferences at real-time on all three devices.

4.2. Validation of Geometric Alignment.

To validate the effectiveness of proposed geometric alignment, we adopt pre-trained VGGFace [28] to embed facial images into feature space and calculate the cosine distance between two distributions. We select 820 images

from the training portrait dataset, which are denoted as I_p , and 820 animation style training samples I_s , and randomly combine them into 820 image pairs. TPS is used to warp I_p in each pair to I_{p2s} and I_s in each pair to I_{s2p} respectively. Feature distances are calculated between each image pair and averaged among the full dataset. From the results shown in table 3, we can find the distances between I_p and I_{s2p} and between I_s and I_{p2s} are smaller than the distance between I_s and I_p . This clearly demonstrates the proposed geometric alignment effectively closes the gap between portrait and style distributions.

4.3. Qualitative Comparison

We show the comparison between our proposed method and previous methods in Figure 6. **CycleGAN** effectively stylizes portraits for animation and oil-paint style, but causes deformation such as the hair area in animation style and unclear artifacts in oil-paint style. For water-color and ink-paint style, it suffers from severe mode-collapse due to the limited number of style samples. **AgileGAN** successfully synthesizes visual-pleasant results for animation, water-color and oil-paint style, but fail to preserve the identity and background information and is unable to generate meaningful results for ink-paint style. **U-GAT-IT** synthe-



Figure 7. Results of models trained with different amount of style samples. Column b, c, d, e represent models trained with 100, 200, 400 and 800 style samples respectively

Table 4. Performance evaluated by Art-FID of models trained with different amount of style samples.

Style samples	100	200	400	800
Art-FID	83.86	93.52	80.15	85.80

sizes good quality results in animation style, but the performance drops drastically with the decrease of style sample. It fails to preserve the identity in the watercolor style and even the face pose in the ink paint style. The results of **DRIT++** are greatly influenced by the style examples in all presented styles. Especially in water-color and ink-paint style, it fails to preserve the identity information of the portraits and synthesis results almost the same as style example.

Our proposed method, on the contrary, synthesizes visually pleasant stylization results for both 4 styles, because the proposed geometric alignment effectively align the key areas and help the model learn style information of corresponding regions. It also preserves identity, gender, age and even background information, as the geometric aligned cycle-consistent loss effectively constrains the spatial information. To conclude, our method outperforms previous methods in better stylization quality, fewer artifacts, preservation of identity and stability on small training dataset.

4.4. Quantitative evaluation

Art-FID is a modification version of FID (Fréchet Inception Distance) [7] designed to quantitatively evaluate the performance of style transfer tasks. An image classification network [37] is trained on a large-scale artwork dataset and used to extract high-level features of images to calculate the distance between two distributions. In this work, it is adopted to evaluate the performance of previous methods and our method. As is shown in table 2, our large model and small model achieves 1st and 2nd place in animation and watercolor style. In oil painting and ink painting style, our large model achieved the 1st in Art-FID and our small model are ranked the 3rd, with small gap to the 2nd, indicating that our method synthesizes results similar to style

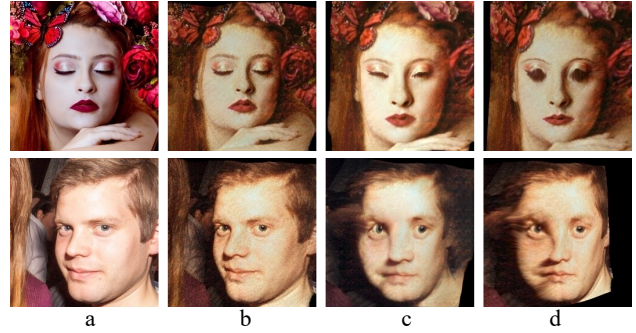


Figure 8. Comparison of spatial editing. a: the input portrait images. b: stylization result without spatial deformation. c: stylization with spatial deformation in the feature space. d: stylization with spatial deformation in the pixel space (by directly applying TPS on results in b).

examples and also achieves good stylization ability.

4.5. Analysis of the Scale of Style Samples

We train our model with 100, 200, 400 and 800 animation style samples respectively to explore the influence of the scale of style dataset. As is shown in Figure 7, reducing the number of training samples causes decreased synthesis quality and more artifacts on the eyes and eyebrow areas, but the overall information such as haircut, face position, gender, age and identity are still preserved. The quantitative results evaluated by Art-FID of each model are shown in Table 4, where the scores fluctuate in a small range. This is because the geometric align framework allows the network to learn to stylize from the corresponding area, which improved efficiency and reduced artifacts caused by mismatch, facilitated few-shot learning. The Art-FID of each model is not in descending order as the number of style samples increases, which is likely due to the randomness caused by the limited number of image pairs used to calculate Art-FID.

4.6. Analysis of Spatial Deformation Editing

The comparison of spatial deformation editing is shown in figure 8, where 8 a shows the input portrait images, 8 b shows the stylization result without spatial deformation, 8 c represents stylization with spatial deformation in the feature space, and 8 d illustrate the spatial editing in the pixel space by directly apply TPS on the result of 8 b.

Directly applying TPS on images leads to artifacts on eye regions or blurred face edges in figure 8 d, which are common side-effects of TPS. Our proposed methods shown in 8 c, on the contrary, improves the editing quality and synthesize images with clear edges and fine details. This is because the TPS deformations applied in low resolution feature space decrease the pixel errors, and the following trainable layers further learn to reduce the errors and generate clear and sharp images from the dataset.

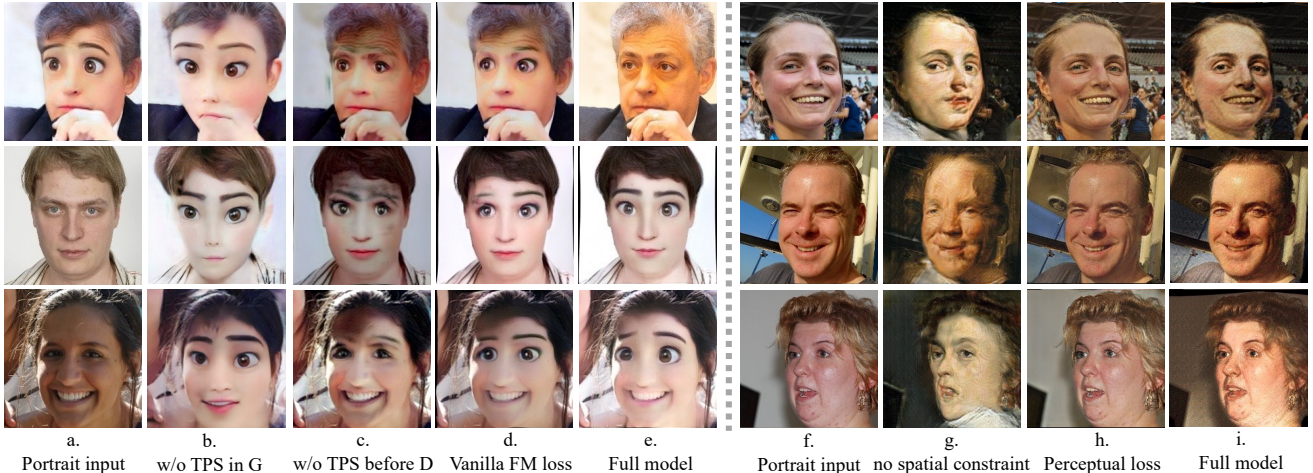


Figure 9. Component analysis by ablating or changing each module

4.7. Components Analysis

Analysis of **TPS based geometric alignment** is shown in figure 9a-e. Ablating TPS module in the generator results in severe distortions of face shape in figure 9b, as the generator without TPS is not able to control the spatial deformation. Ablating TPS based alignment before discriminator causes color changes and messy textures in the forehead regions in figure 9c, due to the unaligned image pairs bring in confusing information. Adopting vanilla feature matching loss leaves artifacts on eye regions in figure 9d, because the lack of spatial information deteriorates the model’s discriminative ability. The proposed full pipeline in figure 9e can synthesize results in apparent animation style with clean textures and sharp edges, because the TPS modules in both generator and discriminator semantically align the training pairs, enable networks to focus on corresponding regions and avoided distortions caused by misalignments.

We show the comparison between different **Deformation invariant constraints** in figure 9f-i. In figure 9g, ablating spatial constraints caused artifacts on the skin areas, because the generator lack spatial control during training. Figure 9h shows results synthesized with perceptual loss, which present little oil-paint style. The reason is that perceptual loss imposes too strong constraint on all pixels evenly, deteriorating the stylization effects. Figure 9i shows the results of our proposed method with clear oil-paint styles and textures, and little artifacts and distortions. This is because the spatial correlative loss learns to preserving scene structure consistency while allowing appearance changes on import regions such as eyes, mouth and noses.

4.8. User Study

The evaluation of portrait stylization is highly subjective and easily influenced by individual preference. We thus adopt user studies to demonstrate how users evaluate our method and previous methods. 30 participants are asked to

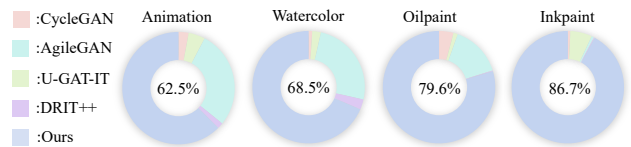


Figure 10. Result of user study. The proportion of user preferring our method is indicated by the percentage in the pie chart.

select the results with the best stylization quality and preserves the person’s identity. Each participant was shown 64 image sets, with 16 sets for each style, and the results of our method and 4 previous methods in each set.

We show the result of user study in figure 10, where over 60% of users select our method as the best, which indicates significant superiority over compared methods in synthesis quality. We also notice that, our methods receives lowest preference rate in animation style with the largest style training set and highest preference rate in ink-paint style with the smallest style training set. This demonstrates that the advantage of our methods becomes more obvious when the number of training style samples decreases, further confirming the few-shot leaning capability of our method.

5. Conclusions

We propose a portrait stylization method that could be trained with limited style examples and inference at real-time on mobile devices. Geometric alignment is adopted to close the gap between portrait and style domains by integrating the TPS in both generation and discrimination process, enabling the framework to be trained in a semantic aligned manner. The method synthesizes high-quality stylization results that outperforms previous methods in qualitative comparison, quantitative evaluation and user study. Ablation study is also conducted to demonstrate the influence of each component.

References

- [1] Fred L. Bookstein. Principal warps: Thin-plate splines and the decomposition of deformations. *IEEE Transactions on pattern analysis and machine intelligence*, 11(6):567–585, 1989. [2](#), [4](#)
- [2] Yang Chen, Yu-Kun Lai, and Yong-Jin Liu. Cartoongan: Generative adversarial networks for photo cartoonization. In *Proceedings of the IEEE Conference on Computer Vision and Pattern Recognition*, pages 9465–9474, 2018. [2](#), [3](#)
- [3] Prafulla Dhariwal and Alexander Nichol. Diffusion models beat gans on image synthesis. *Advances in Neural Information Processing Systems*, 34:8780–8794, 2021. [3](#)
- [4] Leon A Gatys, Alexander S Ecker, and Matthias Bethge. A neural algorithm of artistic style. *arXiv preprint arXiv:1508.06576*, 2015. [1](#), [2](#)
- [5] Ian Goodfellow, Jean Pouget-Abadie, Mehdi Mirza, Bing Xu, David Warde-Farley, Sherjil Ozair, Aaron Courville, and Yoshua Bengio. Generative adversarial nets. In *Advances in Neural Information Processing Systems*, pages 2672–2680, 2014. [1](#), [3](#)
- [6] Aaron Hertzmann. Painterly rendering with curved brush strokes of multiple sizes. In *Proceedings of the 25th annual conference on Computer graphics and interactive techniques*, pages 453–460, 1998. [2](#)
- [7] Martin Heusel, Hubert Ramsauer, Thomas Unterthiner, Bernhard Nessler, and Sepp Hochreiter. Gans trained by a two time-scale update rule converge to a local nash equilibrium. *Advances in neural information processing systems*, 30, 2017. [7](#)
- [8] Jonathan Ho, Ajay Jain, and Pieter Abbeel. Denoising diffusion probabilistic models. *Advances in Neural Information Processing Systems*, 33:6840–6851, 2020. [2](#), [3](#)
- [9] Xun Huang, Ming-Yu Liu, Serge Belongie, and Jan Kautz. Multimodal unsupervised image-to-image translation. In *Proceedings of the European Conference on Computer Vision (ECCV)*, pages 172–189, 2018. [3](#)
- [10] Andrey Ignatov, Nikolay Kobyshev, Radu Timofte, Kenneth Vanhoey, and Luc Van Gool. Wespe: weakly supervised photo enhancer for digital cameras. In *Proceedings of the IEEE Conference on Computer Vision and Pattern Recognition Workshops*, pages 691–700, 2018. [3](#)
- [11] Phillip Isola, Jun-Yan Zhu, Tinghui Zhou, and Alexei A Efros. Image-to-image translation with conditional adversarial networks. In *Proceedings of the IEEE Conference on Computer Vision and Pattern Recognition*, pages 1125–1134, 2017. [2](#), [3](#)
- [12] Justin Johnson, Alexandre Alahi, and Li Fei-Fei. Perceptual losses for real-time style transfer and super-resolution. In *European Conference on Computer Vision*, pages 694–711. Springer, 2016. [1](#), [2](#), [3](#)
- [13] Tero Karras, Miika Aittala, Janne Hellsten, Samuli Laine, Jaakko Lehtinen, and Timo Aila. Training generative adversarial networks with limited data. *Advances in Neural Information Processing Systems*, 33:12104–12114, 2020. [5](#)
- [14] Tero Karras, Samuli Laine, and Timo Aila. A style-based generator architecture for generative adversarial networks. In *Proceedings of the IEEE/CVF conference on computer vision and pattern recognition*, pages 4401–4410, 2019. [2](#), [3](#), [5](#)
- [15] Tero Karras, Samuli Laine, Miika Aittala, Janne Hellsten, Jaakko Lehtinen, and Timo Aila. Analyzing and improving the image quality of stylegan. In *Proceedings of the IEEE/CVF conference on computer vision and pattern recognition*, pages 8110–8119, 2020. [2](#), [3](#)
- [16] Junho Kim, Minjae Kim, Hyeonwoo Kang, and Kwanghee Lee. U-gat-it: Unsupervised generative attentional networks with adaptive layer-instance normalization for image-to-image translation. *arXiv preprint arXiv:1907.10830*, 2019. [5](#)
- [17] Diederik Kingma, Tim Salimans, Ben Poole, and Jonathan Ho. Variational diffusion models. *Advances in neural information processing systems*, 34:21696–21707, 2021. [3](#)
- [18] Diederik P Kingma and Jimmy Ba. Adam: A method for stochastic optimization. *arXiv preprint arXiv:1412.6980*, 2014. [5](#)
- [19] Diederik P Kingma and Max Welling. Auto-encoding variational bayes. *arXiv preprint arXiv:1312.6114*, 2013. [3](#)
- [20] Jan Eric Kyprianidis and Jürgen Döllner. Image abstraction by structure adaptive filtering. In *TPCG*, pages 51–58, 2008. [2](#)
- [21] Hsin-Ying Lee, Hung-Yu Tseng, Jia-Bin Huang, Maneesh Singh, and Ming-Hsuan Yang. Diverse image-to-image translation via disentangled representations. In *Proceedings of the European Conference on Computer Vision (ECCV)*, pages 35–51, 2018. [3](#)
- [22] Hsin-Ying Lee, Hung-Yu Tseng, Qi Mao, Jia-Bin Huang, Yu-Ding Lu, Maneesh Singh, and Ming-Hsuan Yang. Dri++: Diverse image-to-image translation via disentangled representations. *International Journal of Computer Vision*, 128(10):2402–2417, 2020. [5](#)
- [23] Yijun Li, Chen Fang, Aaron Hertzmann, Eli Shechtman, and Ming-Hsuan Yang. Im2pencil: Controllable pencil illustration from photographs. In *Proceedings of the IEEE/CVF Conference on Computer Vision and Pattern Recognition*, pages 1525–1534, 2019. [3](#)
- [24] Jing Liao, Yuan Yao, Lu Yuan, Gang Hua, and Sing Bing Kang. Visual attribute transfer through deep image analogy. *arXiv preprint arXiv:1705.01088*, 2017. [2](#)
- [25] Songhua Liu, Tianwei Lin, Dongliang He, Fu Li, Ruifeng Deng, Xin Li, Errui Ding, and Hao Wang. Paint transformer: Feed forward neural painting with stroke prediction. In *Proceedings of the IEEE/CVF international conference on computer vision*, pages 6598–6607, 2021. [2](#)
- [26] Cewu Lu, Li Xu, and Jiaya Jia. Combining sketch and tone for pencil drawing production. In *Proceedings of the Symposium on Non-Photorealistic Animation and Rendering*, pages 65–73. Eurographics Association, 2012. [2](#)
- [27] Kiri Nichol. Painter by numbers, wikiart. *Kiri Nichol*, 2016. [5](#)
- [28] Omkar M Parkhi, Andrea Vedaldi, and Andrew Zisserman. Deep face recognition. 2015. [6](#)
- [29] Adam Paszke, Sam Gross, Francisco Massa, Adam Lerer, James Bradbury, Gregory Chanan, Trevor Killeen, Zeming

- Lin, Natalia Gimelshein, Luca Antiga, et al. Pytorch: An imperative style, high-performance deep learning library. *Advances in neural information processing systems*, 32, 2019. 5
- [30] Deepak Pathak, Philipp Krahenbuhl, Jeff Donahue, Trevor Darrell, and Alexei A Efros. Context encoders: Feature learning by inpainting. In *Proceedings of the IEEE Conference on Computer Vision and Pattern Recognition*, pages 2536–2544, 2016. 3
- [31] Justin NM Pinkney and Doron Adler. Resolution dependent gan interpolation for controllable image synthesis between domains. *arXiv preprint arXiv:2010.05334*, 2020. 2
- [32] Artsiom Sanakoyeu, Dmytro Kotovenko, Sabine Lang, and Bjorn Ommer. A style-aware content loss for real-time hd style transfer. In *Proceedings of the European Conference on Computer Vision (ECCV)*, pages 698–714, 2018. 2, 3
- [33] Ahmed Selim, Mohamed Elgharib, and Linda Doyle. Painting style transfer for head portraits using convolutional neural networks. *ACM Transactions on Graphics (TOG)*, 35(4):1–18, 2016. 1
- [34] YiChang Shih, Sylvain Paris, Connelly Barnes, William T Freeman, and Frédo Durand. Style transfer for headshot portraits. 2014. 2
- [35] Guoxian Song, Linjie Luo, Jing Liu, Wan-Chun Ma, Chunpong Lai, Chuanxia Zheng, and Tat-Jen Cham. Agilegan: stylizing portraits by inversion-consistent transfer learning. *ACM Transactions on Graphics (TOG)*, 40(4):1–13, 2021. 5
- [36] Yang Song and Stefano Ermon. Generative modeling by estimating gradients of the data distribution. *Advances in Neural Information Processing Systems*, 32, 2019. 2, 3
- [37] Christian Szegedy, Vincent Vanhoucke, Sergey Ioffe, Jon Shlens, and Zbigniew Wojna. Rethinking the inception architecture for computer vision. In *Proceedings of the IEEE conference on computer vision and pattern recognition*, pages 2818–2826, 2016. 7
- [38] Aneta Texler, Ondřej Texler, Michal Kučera, Menglei Chai, and Daniel Šykora. Faceblit: Instant real-time example-based style transfer to facial videos. *Proceedings of the ACM on Computer Graphics and Interactive Techniques*, 4(1):1–17, 2021. 2
- [39] Bin Wang, Wenping Wang, Huaiping Yang, and Jiaguang Sun. Efficient example-based painting and synthesis of 2d directional texture. *IEEE Transactions on Visualization and Computer Graphics*, 10(3):266–277, 2004. 2
- [40] Jue Wang, Yingqing Xu, Heung-Yeung Shum, and Michael F Cohen. Video tooning. In *ACM Transactions on Graphics (ToG)*, volume 23, pages 574–583. ACM, 2004. 2
- [41] Ting-Chun Wang, Ming-Yu Liu, Jun-Yan Zhu, Andrew Tao, Jan Kautz, and Bryan Catanzaro. High-resolution image synthesis and semantic manipulation with conditional gans. In *Proceedings of the IEEE conference on computer vision and pattern recognition*, pages 8798–8807, 2018. 2
- [42] Xinrui Wang and Jinze Yu. Learning to cartoonize using white-box cartoon representations. In *Proceedings of the IEEE/CVF conference on computer vision and pattern recognition*, pages 8090–8099, 2020. 2, 3
- [43] Matthias Wright and Björn Ommer. Artfid: Quantitative evaluation of neural style transfer. In *DAGM German Conference on Pattern Recognition*, pages 560–576. Springer, 2022. 5
- [44] Yue Wu and Qiang Ji. Facial landmark detection: A literature survey. *International Journal of Computer Vision*, 127(2):115–142, 2019. 2
- [45] Li Xu, Cewu Lu, Yi Xu, and Jiaya Jia. Image smoothing via l0 gradient minimization. In *ACM Transactions on Graphics (TOG)*, volume 30, page 174. ACM, 2011. 2
- [46] Ming Yang, Shu Lin, Ping Luo, Liang Lin, and Hongyang Chao. Semantics-driven portrait cartoon stylization. In *Proceedings of IEEE International Conference on Image Processing*, pages 1805–1808. IEEE, 2010. 2
- [47] Shuai Yang, Liming Jiang, Ziwei Liu, and Chen Change Loy. Pastiche master: Exemplar-based high-resolution portrait style transfer. In *Proceedings of the IEEE/CVF Conference on Computer Vision and Pattern Recognition*, pages 7693–7702, 2022. 2
- [48] Jordan Yaniv, Yael Newman, and Ariel Shamir. The face of art: landmark detection and geometric style in portraits. *ACM Transactions on graphics (TOG)*, 38(4):1–15, 2019. 2
- [49] Lvmin Zhang, Chengze Li, Edgar Simo-Serra, Yi Ji, Tien-Tsin Wong, and Chunping Liu. User-guided line art flat filling with split filling mechanism. In *Proceedings of the IEEE/CVF conference on computer vision and pattern recognition*, pages 9889–9898, 2021. 3
- [50] Lvmin Zhang, Chengze Li, Tien-Tsin Wong, Yi Ji, and Chunping Liu. Two-stage sketch colorization. *ACM Transactions on Graphics (TOG)*, 37(6):1–14, 2018. 3
- [51] Richard Zhang, Phillip Isola, and Alexei A Efros. Colorful image colorization. In *European Conference on Computer Vision*, pages 649–666. Springer, 2016. 3
- [52] Richard Zhang, Phillip Isola, Alexei A Efros, Eli Shechtman, and Oliver Wang. The unreasonable effectiveness of deep features as a perceptual metric. In *Proceedings of the IEEE conference on computer vision and pattern recognition*, pages 586–595, 2018. 5
- [53] Chuanxia Zheng, Tat-Jen Cham, and Jianfei Cai. The spatially-correlative loss for various image translation tasks. In *Proceedings of the IEEE/CVF Conference on Computer Vision and Pattern Recognition*, pages 16407–16417, 2021. 2
- [54] Xingran Zhou, Bo Zhang, Ting Zhang, Pan Zhang, Jianmin Bao, Dong Chen, Zhongfei Zhang, and Fang Wen. Cocosnet v2: Full-resolution correspondence learning for image translation. In *Proceedings of the IEEE/CVF Conference on Computer Vision and Pattern Recognition*, pages 11465–11475, 2021. 2
- [55] Jun-Yan Zhu, Taesung Park, Phillip Isola, and Alexei A Efros. Unpaired image-to-image translation using cycle-consistent adversarial networks. In *Proceedings of IEEE International Conference on Computer Vision*, 2017. 2, 3, 5
- [56] Zhengxia Zou, Tianyang Shi, Shuang Qiu, Yi Yuan, and Zhenwei Shi. Stylized neural painting. In *Proceedings of the IEEE/CVF Conference on Computer Vision and Pattern Recognition*, pages 15689–15698, 2021. 2